Article

Journal of
Nanoscience and Nanotechnology
Vol. 15, 2628–2633, 2015
www.aspbs.com/jnn

Optimization of Polydiacetylene-Coated Superparamagnetic Magnetite Biosensor for Colorimetric Detection of Biomarkers

Terence Chan[1,2,†], Mohit S. Verma[1,2,†], and Frank X. Gu[1,2,*]

[1] Department of Chemical Engineering, [2] Waterloo Institute for Nanotechnology,
University of Waterloo, Waterloo, ON, N2L3G1, Canada

Biosensors for point-of-care testing of critical illnesses are urgently needed, especially in many areas of poor healthcare infrastructure. Polydiacetylene-based sensors are ideal because of their unique colorimetric properties where blue to red color shifts can be observed with the naked eye. In this work, a colorimetric biosensor capable of simple, rapid magnetic separation is optimized, using horse IgG as a model antibody, to obtain higher sensitivity. Composed of a unique combination of polydiacetylene and superparamagnetic iron oxide, the biosensor is fabricated at varying ratios of polydiacetylene to demonstrate optimization of color responsiveness. At increasing polydiacetylene ratios, improved color responsiveness and aqueous dispersion are observed, but the magnetic separation efficiency starts to suffer. The optimal color response is obtained at 90 wt% polydiacetylene. In addition, a 50 times improved lower detection limit of 0.01 mg/mL horse IgG is achieved, a relevant biomarker concentration for diagnosing sepsis. This platform provides a promising colorimetric biosensor for point-of-care use.

Keywords: Point-of-Care Testing, Polydiacetylene, Colorimetric Biosensor, Superparamagnetic Iron Oxide, Sepsis.

1. INTRODUCTION

Biosensors capable of satisfying the demands of point-of-care testing (POCT) applications are becoming urgently needed for the diagnosis of critical illnesses, such as tuberculosis,[1] HIV,[2] and sepsis.[3] The demand for these sensors is strong in typical clinical settings,[4] but are crucial in areas of poor healthcare infrastructure, a widespread issue in many developing nations.[5] Colorimetric biosensors, especially those based on polydiacetylene (PDA), have garnered increasing attention as a biosensor platform because of their ability of displaying a sharp blue to red color transition in response to receptor-ligand interactions. Previous examples include calixarene-protein,[6] antibody-antigen,[7] and glycolipid-bacteria[8] binding, demonstrating the versatility and potential wide-ranging uses of PDA-based sensors.

Existing PDA-based sensors utilize either thin-film structures requiring solid supports such as glass,[9] sol–gels[10] and cellulose,[11] or solution-based liposome structures.[12,13] For biosensor applications, solution-based structures offer several advantages over solid-state structures, including increased surface area for detection,[14] increased probability of sensor-analyte interaction and preservation of native analyte form and function.[15] However, existing solution-based approaches are impractical for POCT applications because they can only use purified, single target samples and liposome separation is not possible without specialized laboratory equipment.

A recent advancement in solution-based PDA sensors demonstrated successful colorimetric detection after immobilizing PDA on silica microbeads.[14] This system is extremely useful for flow cytometry applications, but inherently requires extensive sample preparation, complex laboratory equipment, and specialized technical training for operation and data analysis, conflicting with POCT prerequisites. To address these issues, a colorimetric, superparamagnetic biosensor[16] for biomarker detection is optimized for enhanced sensitivity in this work, combining the benefits of PDA-based sensing and the simple, rapid

*Author to whom correspondence should be addressed.
†These two authors contributed equally to this work.

 1533-4880/2015/15/2628/006 doi:10.1166/jnn.2015.10219

magnetic separation of captured targets requiring only a common magnet. The biosensor is surface functionalized with antibodies to study its colorimetric properties. The amount of PDA added to the biosensor determines the degree of color change as well as the ease of magnetic separation of the particles. This work demonstrates optimization of the biosensor in regards to these two competing parameters which provides a magnetically separable biosensor with color change visible to the naked eye.

2. EXPERIMENTAL DETAILS

2.1. Materials

10,12-Pentacosadiynoic acid (PCDA) was purchased from Alfa Aesar and purified with 0.45 μm polytetrafluoroethylene membrane filter before use. (*S*)-*N*-(5-Amino-1-carboxypentyl)iminodiacetic acid, *cis*-9-octadecenoic acid, 1-ethyl-3-(3-dimethylaminopropyl) carbodiimide (EDC), 1-hydroxy-2,5-pyrrolidinedione (NHS), hydroxy-2,5-dioxopyrrolidine-3-sulfonicacid sodium salt (sulfo-NHS), and 2-aminoethanol purchased from Sigma Aldrich (Canada), NaCl, $FeCl_2$, and $Fe_2(SO_4)_3$ purchased from Fisher Scientific (Canada), and *N*,*N*-diethylethanamine (TEA), NH_4OH, HCl, $CHCl_3$, tetrahydrofuran (THF), and ethanol purchased from EMD Millipore were used as received. All solvents used were HPLC grade. Horse IgG and rabbit anti-horse IgG antibodies were purchased from Rockland Immunochemicals Inc. and washed with sterile PBS buffer (0.1 M sodium phosphate, 0.15 M NaCl, pH 7.2) using Amicon Ultra-15 10 K centrifugal filter units from EMD Millipore before use. Transmission electron microscopy (TEM) images were obtained using a Philips CM10 microscope.

2.2. Synthesis of Hydrophobic SPIONs and Amphiphilic PCDA

Oleic acid-coated SPIONs (OA-SPIONs) were synthesized similar to a previously described coprecipitation method,[17] using excess oleic acid to achieve a hydrophobic coating. Amphiphilic PDA (Lys-PCDA) were synthesized via EDC/NHS conjugation chemistry, reacting NHS-activated PCDA in THF with a 1.2 molar excess of (*S*)-*N*-(5-amino-1-carboxypentyl)iminodiacetic acid in Milli-Q water adjusted to ~pH 9 with TEA.

2.3. Biosensor Fabrication

Functionalized amphiphilic PDA-coated SPION sensors (Lys-PCDA/SPIONs) were fabricated at various weight percentages (wt%) of Lys-PCDA ranging from 60–95 wt% while keeping constant the amount of OA-SPIONs using the concept of nanoprecipitation. Briefly, Lys-PCDA and OA-SPIONs were mixed in THF and added dropwise to Milli-Q water at 12 mL/h under mechanical stirring, stirred for 20 minutes, then washed using magnetic separation. Sensors were functionalized with equal amounts of anti-horse IgG antibody according to the molar

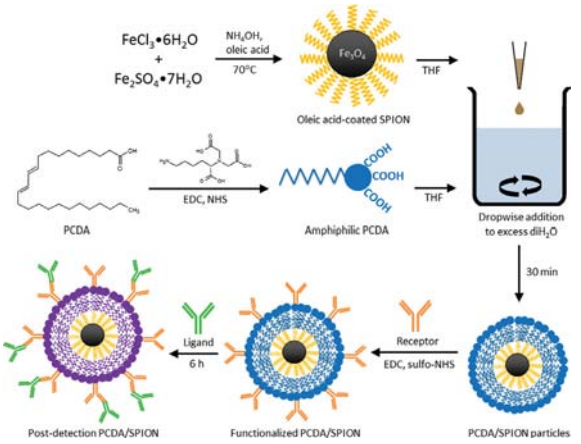

Scheme 1. Schematic illustration of the PCDA/SPION biosensor synthesis and operation.

fraction of Lys-PCDA in each wt% sample, via two-step EDC/sulfo-NHS conjugation in PBS buffer. Unreacted sulfo-NHS was blocked with 2-aminoethanol. Fabrication was completed with irradiation at 254 nm in 3 bursts of 1 mJ/cm^2.

2.4. Antibody Assay

Equal aliquots of each wt% sample of Lys-PCDA/SPIONs were incubated with 4 mL of 0, 0.01, 0.1, 0.5, and 1 mg/mL horse IgG in PBS buffer and mixed at room temperature with gentle orbital shaking until marked color changes were observed (6 hours).

The synthesis paths of the functionalized core–shell PCDA/SPION biosensor are shown in Scheme 1.

2.5. Characterization

The antibody assay was monitored at set time intervals for the appearance of color change and photographed at each interval in a controlled white-surfaced digital photo box with identical lighting and camera settings. UV-visible absorption measurements were recorded at the end of the antibody incubation with a Biotek Epoch spectrophotometer using Greiner Bio-One UV-Star 96-well microplates. Lys-PCDA/SPIONs were washed 3 times with PBS buffer before spectroscopic analysis to remove any interference effects from the horse IgG solution. Spectra with a wavelength range of 400 to 700 nm, in 10 nm increments, were recorded. The color transition was quantified as a colorimetric response (CR %), using the following:[7]

$$CR\ \% = \frac{(PB_0 - PB_1)}{PB_0} \times 100\%$$

where $PB = A_{blue}/(A_{blue} + A_{red})$, A was the UV-visible absorbance value of the particle's "blue" state at 650 nm or the "red" state at 540 nm, and PB_0 and PB_1 were the respective colorimetric ratios of the particles before and after the assay.

The images obtained for the antibody assay were cropped to 200×200 pixels squares and then the color was measured for each image using the Hue, Saturation and Value (HSV) model in MathWorks© MATLAB®. The saturation component were found to correspond closely to the visually observed color change and hence this component was used to quantify the degree of color change observed. Each of the saturation values was normalized by subtracting the initial values and also any decrease in saturation observed after washing of the particles. The analysis was conducted for all time points and maximum saturation change is reported here.

3. RESULTS AND DISCUSSION

3.1. Characterization of Sensor Fabrication

The objective of this work was to fabricate a colorimetric, magnetically separable sensor capable of demonstrating an optimized color response, by varying the ratio of amphiphilic PDA to hydrophobic SPIONs during sensor fabrication. The size of SPIONs determines their superparamagnetic properties and hence TEM was used to characterize the particles after modification with Lys-PCDA. Figure 1(a) shows that the particle sizes are in the range of 6–14 nm with an average size of about 10 nm. Since these are below 20 nm, the superparamagnetic properties of the SPIONs are maintained. Normalized absorption spectra and visual comparisons of the sensors in the presence of ethanol are shown in Figures 1(b)–(e) and clearly demonstrate the effects of increasing the amount of PDA, which are three-fold. First, increasing the amount of PDA results in distinct increases in the initial blue color, as well as a greater color response when perturbed with ethanol (Figs. 1(b)–(d)), which has been previously reported to swell PDA surfaces and affect a transition to the "red" state.[18] For example, sensors composed of 95 wt% PDA demonstrated a 23.054% colorimetric response compared to a 0.678% response from 60 wt% PDA sensors (Fig. 1(e)).

Second, increasing the amount of PDA assists in shielding the UV-visible absorption interference caused by the black SPION cores, up to 90 wt% PDA, indicated by the absorbance values between 400–600 nm. Previous free-floating PDA vesicles have demonstrated decreasing absorption values from ~590 nm to 400 nm.[19] In comparison, the Lys-PCDA/SPIONs do not display this trend. At lower PDA wt%, especially noticeable among 60–75 wt%, the PDA surface coating is not thick enough to reduce absorption by the SPION core. However, it is important to note that this interference does not affect the "red" state reading at 540 nm if enough PDA is used during fabrication, indicated by the marked peaks at 540 nm among the 75–95 wt% PDA sensors (Fig. 1(d)).

Third, increasing the amount of PDA greatly improves the aqueous dispersion of the Lys-PCDA/SPION sensors. This is visually demonstrated by the denser solutions at

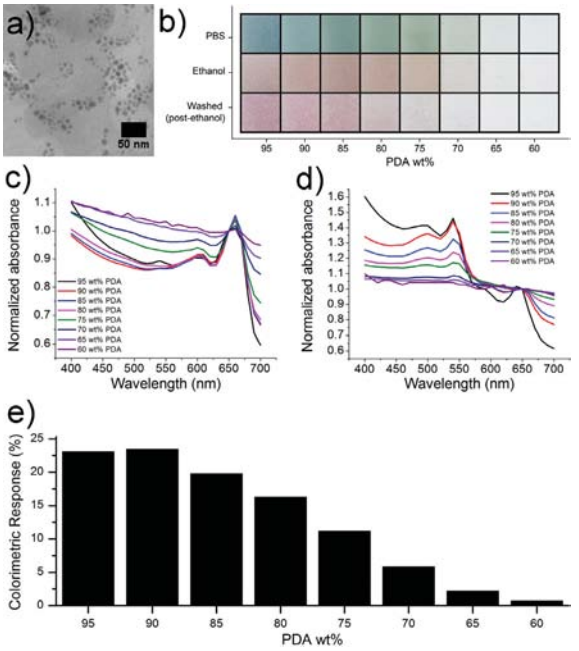

Figure 1. Characterization of Lys-PCDA/SPION sensors: (a) Transmission electron microscope (TEM) image of Lys-PCDA/SPION (b) Photographs of varying PDA wt% sensors. (c) Absorption spectra in PBS. (d) Absorption spectra post-ethanol. (e) Colorimetric response of sensors to ethanol.

higher PDA wt%, in comparison to the increasingly clear solutions at 60–70 wt% PDA (Fig. 1(b)). During wash steps of biosensor fabrication, the lower wt% sensor particles were observed to preferentially float at the surface of the aqueous solutions. This prevented efficient magnetic separation and retention of the Lys-PCDA/SPIONs, resulting in the loss of sensor particles (not shown). However, very high wt% was also observed to be undesirable, specifically at 95 and 90 wt% PDA. During wash steps, these sensors required longer separation times, and a small fraction of these sensor particles were observed in wash run-off, particularly the 95 wt% Lys-PCDA/SPIONs. It is highly suspected that the thicker non-magnetic PDA coatings reduced the net saturation magnetization (defined as the magnetic moment per mass or volume of a material) of the SPION cores by increasing the mass per particle without contributing to the magnetic properties, which led to lower magnetic separability. It has been previously shown that magnetic separation of SPIONs is dependent upon the concentration and aggregation of the magnetic material in the net system.[20, 21] Thus, increasing the amount of non-magnetic material between SPIONs, such as found in the high wt% PDA sensors, would also be expected to interfere with the transient aggregation of neighboring SPIONs that allows their separation to occur. This observation coincides with a previous study which found that increasing the amount of non-magnetic material in relation to the amount of hydrophobic SPIONs present in the system resulted in

decreasing net saturation magnetization,[17] which would be expected to reduce their separability.

3.2. Optimization of Colorimetric Sensing Using Antibody-Antigen Assay

To demonstrate the colorimetric response of biomolecule detection, each sensor composition was exposed to varying concentrations of horse IgG solution. As shown in Figure 2, the sensors composed of 85–95 wt% PDA demonstrated the most noticeable color transitions in all four concentrations tested (0.01, 0.1, 0.5, and 1 mg/mL), making a visible transition towards the red state and appearing as the purple color phase after 6 hours. Similar to previous visual observations when tested against ethanol, increasing the wt% of PDA in the sensor resulted in a greater color response to biomolecule detection. However, after washing the sensors for spectrophotometry analysis, 90 and 95 wt% sensors showed reductions in sensor particle retention, with 95 wt% sensors exhibiting less retention than 90 wt%. This is consistent with earlier observations noted above and indicates that utilizing too much PDA can result in suboptimal magnetic separability.

The absorption spectra are shown in Figure 3 and highlight the significance of PDA concentrations used in the sensor fabrication to achieving optimal performance. Spectra for 60–65 wt% appeared very similar to the controls in PBS (Fig. 1(c)), indicating that not enough PDA was present to produce a color response while the 70–75 wt% sensors showed no reliable trends (not shown). This was expected after sensor fabrication, as the 60–75 wt% sensors did not appear as blue as previously described PDA-based sensors. In comparison, 85–95 wt% sensors all showed the appearance of peaks at 540 nm, supporting the visual observations. Of interesting note is that the 90–95 wt% sensors showed the largest peaks at 540 nm among the color response compositions despite the loss of some of the sensor particles during the wash steps. The 85–95 wt% PDA sensors demonstrated a colorimetric response to increasing concentrations of horse IgG. Of significant note is the marked difference between 0 and 0.01 mg/mL and between 0.01 mg/mL and the larger concentrations. In this work, 0.01 mg/mL was specifically chosen to demonstrate the potential applicability of the Lys-PCDA/SPION sensor for biomarker-based diagnosis of critical illnesses such as sepsis. Serum concentrations greater than 0.01 mg/mL of C-reactive protein (CRP), a commonly used biomarker for diagnosing sepsis[22] and several other illnesses,[23] are indicative of sepsis.[24] The 85–95 wt% sensors all demonstrated different colorimetric responses when incubated with 0.01 mg/mL, compared to the higher concentrations of target analyte. Quantitatively, the 85 wt% PDA sensor demonstrated a 2.01% and 1.70% colorimetric response at 0.5 and 0.1 mg/mL when normalized against the colorimetric response at 0.01 mg/mL, while the higher wt% sensors showed 1.48% and 1.42% (for 90 wt% at 0.5 and 0.1 mg/mL), and 1.37% and

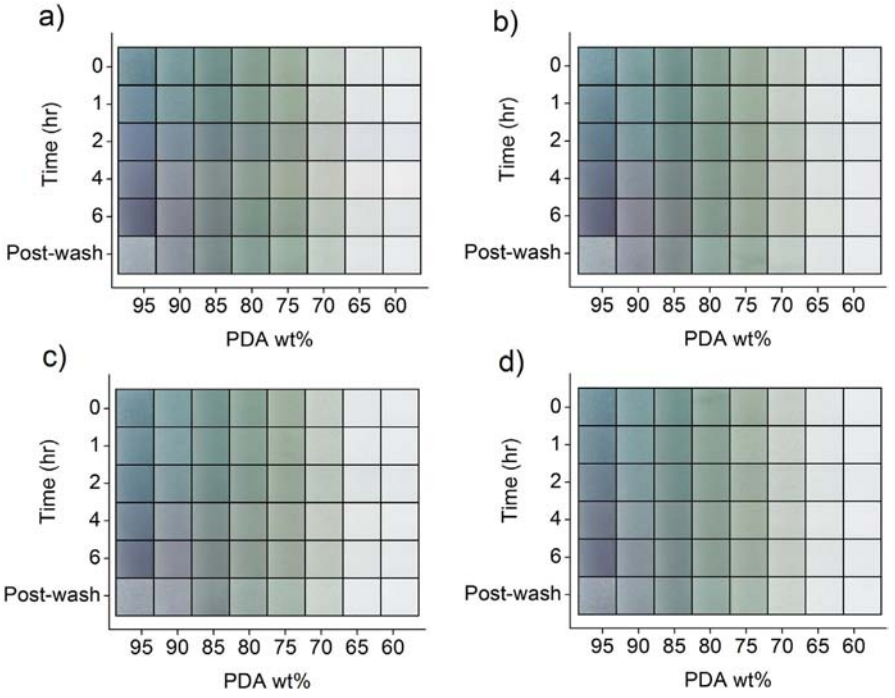

Figure 2. Photographs of Lys-PCDA/SPION sensors of varying PDA wt%, in: (a) 1 mg/mL horse IgG. (b) 0.5 mg/mL horse IgG. (c) 0.1 mg/mL horse IgG. (d) 0.01 mg/mL horse IgG.

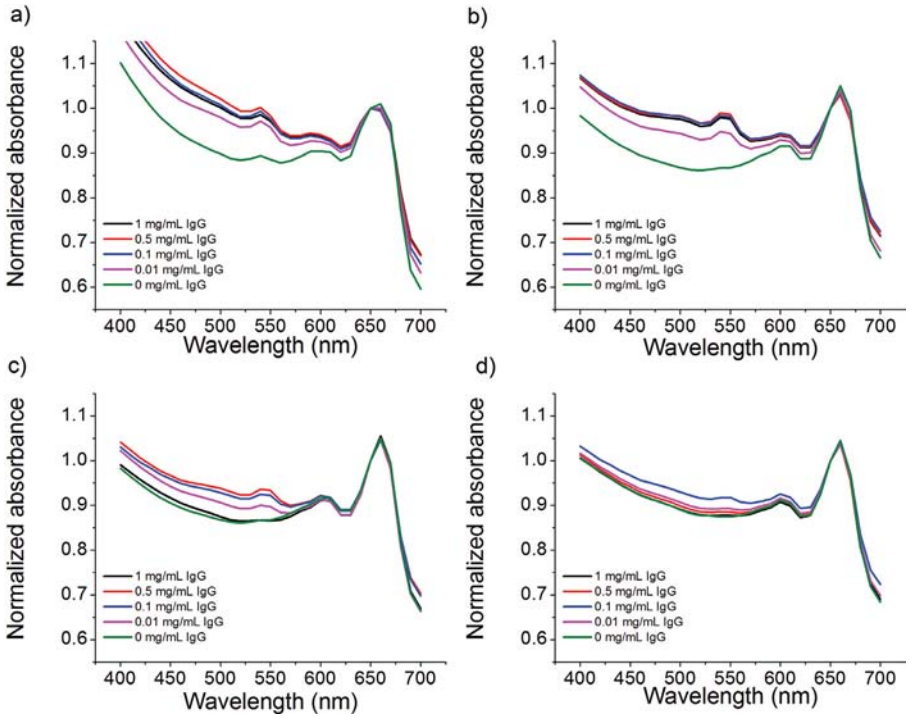

Figure 3. Absorption spectra of Lys-PCDA/SPION sensors of 80–95 wt% PDA, normalized to 650 nm, in increasing horse IgG concentrations: (a) 95 wt% PDA. (b) 90 wt% PDA. (c) 85 wt% PDA. (d) 80 wt% PDA.

1.27% (for 95 wt% at 0.5 and 0.1 mg/mL) colorimetric responses.

In addition to the absorption spectra, the HSV color model was used to quantify the color in the pictures for each of the time points and IgG concentrations and the normalized saturation change was plotted (Fig. 4(a)). The sensor with 90 wt% PDA demonstrated the maximum change in saturation for most of the IgG concentrations and so, it was determined to be the optimal biosensor composition. The kinetics of the 90 wt% PDA sensor in response to 1.0 mg/mL IgG are shown in Figure 4(b), with the normalized saturation change following a sigmoidal curve. The initial lag phase is likely due to a minimum amount of antibodies needed to interact with the antibody receptors on the surface of the biosensor to initiate the color change process in the PDA layer. More than 50% of the change occurred within 3 hours while the color change leveled off after 4 hours. Thus, an incubation time of at least 4 hours is recommended for maximum detection.

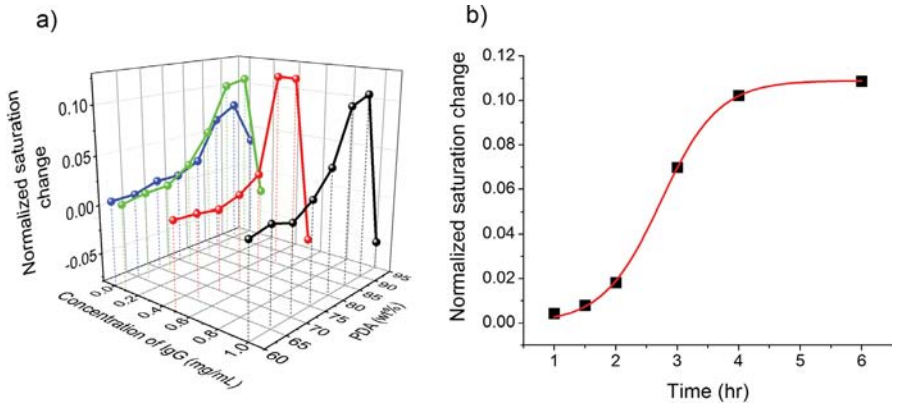

Figure 4. Normalized change in saturation using the HSV model: (a) IgG concentration dependent response of the biosensors with varying amounts of PDA (wt%) (b) kinetics of the optimal biosensor formulation (90 wt% PDA) when exposed to 1 mg/mL IgG.

An optimal magnetically separable biosensor would provide maximum color change with minimal particle loss during the washing steps. Thus, colorimetric response alone is not sufficient to determine the optimal formulation. Based on the results, the optimal ratio of Lys-PCDA to hydrophobic SPIONs to use during sensor fabrication is 90 wt% to achieve highest sensor performance. At PDA ratios below 80 wt%, the sensors demonstrate weak colorimetric sensing properties, likely a result of insufficient amounts of PDA in the system. At lower ratios below 65 wt%, the insufficient amount of Lys-PCDA hinders both the colorimetric sensing and magnetic separability properties. While high ratio of 95 wt% PDA demonstrate greater visual color responsiveness, complete magnetic retention was not observed and the reduction in sensor particles resulted in lower than expected measurable colorimetric responses and normalized saturation changes.

4. CONCLUSIONS

In summary, the colorimetric response of previously described Lys-PCDA/SPION biosensors[16] for point-of-care testing applications was optimized, with the 90 wt% PDA composition showing the best performance. Additionally, the sensors successfully demonstrated a 50 times improved lower detection limit of 0.01 mg/mL, a significant biomarker concentration for diagnosing sepsis.[16] Horse IgG/anti-horse IgG binding was used in this work as a cost-effective optimization of the biosensor and to demonstrate the versatility of the biosensor for detecting different target analytes. The development of the biosensor presented in this work highlights the sensor as a potential diagnostic platform to meet the urgent need of point-of-care testing sensors.

Acknowledgment: This work was financially supported by Natural Sciences and Engineering Research Council of Canada (NSERC) and the Waterloo Institute for Nanotechnology. Mohit S. Verma is grateful for the NSERC Vanier Canada Graduate Scholarship. We would like to thank Tim Leshuk for his feedback on the revisions of this manuscript.

References and Notes

1. F. Drobniewski, V. Nikolayevskyy, Y. Balabanova, D. Bang, and D. Papaventsis, *Int. J. Tuberc. Lung Dis.* 16, 7 (**2012**).
2. S. Mtapuri-Zinyowera, M. Chideme, D. Mangwanya, O. Mugurungi, S. Gudukeya, K. Hatzold, A. Mangwiro, G. Bhattacharya, J. Lehe, and T. Peter, *J. Acquir. Immune Defic. Syndr.* 55, 1 (**2010**).
3. J. U. Becker, C. Theodosis, S. T. Jacob, C. R. Wira, and N. E. Groce, *Lancet Infect. Dis.* 9, 9 (**2009**).
4. U. Sauer, J. Pultar, and C. Preininger, *J. Immunol. Methods* 378, 1 (**2012**).
5. R. W. Peeling and D. Mabey, *Clin. Microbiol. Infect.* 16, 8 (**2010**).
6. S. Kolusheva, R. Zadmard, T. Schrader, and R. Jelinek, *J. Am. Chem. Soc.* 128, 41 (**2006**).
7. S. Kolusheva, R. Kafri, M. Katz, and R. Jelinek, *J. Am. Chem. Soc.* 123, 3 (**2001**).
8. Y. L. Su, J. R. Li, L. Jiang, and J. Cao, *J. Colloid Interface Sci.* 284, 1 (**2005**).
9. Y. Scindia, L. Silbert, R. Volinsky, S. Kolusheva, and R. Jelinek, *Langmuir* 23, 8 (**2007**).
10. I. Gill and A. Ballesteros, *Angew. Chem. Int. Ed. Engl.* 42, 28 (**2003**).
11. A. C. Dos Santos Pires, N. D. F. Ferreira Soares, L. H. Mendes da Silva, Hespanhol da Silva,Maria do Carmo, M. V. De Almeida, M. Le Hyaric, N. J. de Andrade, R. F. Soares, A. B. Mageste, and S. G. Reis, *Sensor Actuat. B-Chem.* 153, 1 (**2011**).
12. J. P. Kim, C. H. Park, and S. J. Sim, *J. Nanosci. Nanotechnol.* 11, 5 (**2011**).
13. A. Perino, A. Klymchenko, A. Morere, E. Contal, A. Rameau, J. Guenet, Y. Mely, and A. Wagner, *Macromol. Chem. Physic.* 212, 2 (**2011**).
14. Q. L. Nie, Y. Zhang, J. Zhang, and M. Q. Zhang, *J. Mater. Chem.* 16, 6 (**2006**).
15. K. Lee, L. K. Povlich, and J. Kim, *Analyst* 135, 9 (**2010**).
16. T. Chan and F. Gu, *Biosens. Bioelectron.* 42, 12 (**2013**).
17. L. Cui, H. Xu, P. He, K. Sumitomo, Y. Yamaguchi, and H. Gu, *J. Polym. Sci. Pol. Chem.* 45, 22 (**2007**).
18. N. Charoenthai, T. Pattanatornchai, S. Wacharasindhu, M. Sukwattanasinitt, and R. Traiphol, *J. Colloid Interface Sci.* 360, 2 (**2011**).
19. S. Kolusheva, E. Wachtel, and R. Jelinek, *J. Lipid Res.* 44, 1 (**2003**).
20. G. De Las Cuevas, J. Faraudo, and J. Camacho, *J. Phys. Chem. C* 112, 4 (**2008**).
21. M. Benelmekki, C. Caparros, A. Montras, R. Goncalves, S. Lanceros-Mendez, and L. M. Martinez, *J. Nanopart. Res.* 13, 8 (**2011**).
22. A. G. Lacour, A. Gervaix, S. A. Zamora, L. Vadas, P. R. Lombard, J. M. Dayer, and S. Suter, *Eur. J. Pediatr.* 160, 2 (**2001**).
23. D. I. Agapakis, D. Tsantilas, P. Psarris, E. V. Massa, P. Kotsaftis, K. Tziomalos, and A. I. Hatzitolios, *Respirology* 15, 5 (**2010**).
24. A. Lannergard, G. Friman, U. Ewald, L. Lind, and A. Larsson, *Acta Paediatr.* 94, 9 (**2005**).

Received: 19 September 2013. Accepted: 22 December 2013.